SCSCL with concomitant restoration of conductivity. Furthermore, SCSCL should be particularly sensitive to electric fields in the crystallographic *c* direction. Thus, with the metal-to-semiconductor transition eliminated via nonperiodic SCSCL, the smooth transition from metal to superconductor becomes possible.[22] So far, the superconducting properties of the available triclinic (TMTSF$_2$X salts can still be explained by an electron–phonon coupling (rather than electron–exciton coupling)[28] BCS theory.

Conclusion

A detailed study of the three-dimensional structure of $(TMTSF)_2AsF_6$ (isomorphous to the PF_6^- and ClO_4^- salts[22]) has led to the conclusion that these salts are pseudo-two dimensional, that there are strong interactions between certain selenium atoms in specific ways (clustering),[29] and that there is a periodic lattice of anions. These anion sheets could stabilize partial separation of positive charges and unpaired electron (spins). This separation can be used to formulate an hypothesis to explain the apparent absence of CDW's in these salts.

Acknowledgment. I am grateful to E. A. Chandross, R. C. Haddon, M. L. Kaplan, T. J. Kistenmacher, P. A. Lee, T. M. Rice, G. A. thomas, and W. M. Walsh for comments and discussions. Special thanks go to D. Nalewajek for crystal preparation.

Supplementary Material Available: A listing of structure factors, a table of positional and thermal parameters and their estimated standard deviations, a table of temperature factor expressions, and a table of torsional angles (21 pages). Ordering information is given on any current masthead page.

---

[28] Gutfreund, H.; Little, W. A., in reference 5d p 279. The problem with their detailed platinum chain model was to establish a realistic way to separate the conducting (platinum spine) electrons from the "polarizable" electrons (ligands around Pt).

[29] A structural correlation with superconductivity ("clustering hypothesis") was recently proposed by: Vandenberg, J. M.; Matthias, B. T. *Science (Washington, D.C.)* **1977**, *198*, 194 for ternary superconductors where there are clusters of atoms separated by intercluster distances which are slightly larger (ca. 20%) than the intracluster distances.

Neophyl Rearrangements in Crystalline Bis(3,3,3-triphenylpropanoyl) Peroxide. 1. Dynamic Studies by EPR[1]

Donald W. Walter and J. Michael McBride*

Contribution from the Department of Chemistry, Yale University, New Haven, Connecticut 06511. *Received November 12, 1980*

Abstract: The neophyl rearrangement of 2,2,2-triphenylethyl radical (T) to 1,1,2-triphenylethyl radical (R) was studied by EPR in photolyzed single crystals of the benzene solvate of bis(3,3,3-triphenylpropanoyl)peroxide (TPPP) and deuterated analogues. Six radical pairs were identified: TT*, TT, TR$_1$, TR$_3$, R$_3$R$_3$, and R$_3$R$_1$, where the asterisk denotes a strained structure and the subscript of R denotes which of the phenyl groups of T participated in rearrangement. No other species were observed by EPR. First-order rate constants and approximate activation parameters were determined for disappearance of each of these radical pairs. The temperatures at which they have a half-life of 1 min are 160, 166, 165, 169, 204, and 256 K, respectively. Three of these reactions involve neophyl rearrangement. They have activation energies of about 10 kcal/mol and are retarded by a factor of 10^2–10^4 as compared to rearrangement in solution. For each thermal rearrangement there is a corresponding photochemical rearrangement which yields the same product. The chromophore responsible for rearrangement has not been identified, but sensitization by neighboring peroxide molecules seems plausible.

It is hardly surprising that a rigid molecular environment can exert strong influence over reactions which require association or separation of independent molecules. Having studied matrix control of a number of reactions of this type,[2] we undertook the present study of the conceptually more subtle influence of matrix over an intramolecular process. This work on ground-state reactions complements the investigations of Scheffer and co-workers on lattice control over unimolecular photochemical rearrangements.[3]

We chose to study the free-radical neophyl rearrangement, because previous work suggested that rearrangement of 2,2,2-triphenylethyl to 1,1,2-triphenylethyl (T → R) might be rapid enough to compete with radical-pair collapse in a crystalline solid.[4]

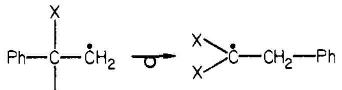

T, X = Ph
N, X = CH$_3$

R, X = Ph
P, X = CH$_3$

From studies at 283–307 K Maillard and Ingold estimated log A (s^{-1}) = 11.7 and E_a = 13.6 kcal/mol for rearrangement of neophyl itself (N → P) in fluid solution.[5] At 163 K, a temperature at which pairs of T radicals in our crystal turn out to collapse only slowly, the half-life of N → P in solution would be about 1 month. Whether because steric hindrance is relieved or because the product radical is conjugated, T rearranges much faster than N. From Kaplan's work on triphenyltin hydride reduction of the

---

[1] Based on the Ph.D. Thesis of D. W. Walter, Yale University, 1980. Presented in part at the 15th Conference on Reaction Mechanisms, Colorado State University, Ft. Collins, CO, June 28, 1974, and at the Fifth International Symposium on Chemistry of the Organic Solid State,, Brandeis University, Waltham, MA, June 13-16, 1978.

[2] (a) Jaffe, A. B.; Skinner, K. J.; McBride, J. M. *J. Am. Chem. Soc.* **1972**, *94*, 8515. (b) Skinner, K. J.; Blaskiewicz, R. J.; McBride, J. M. *Isr. J. Chem.* **1972**, *10*, 457. (c) Karch, N. J.; Koh, E. T.; Whitsel, B. L.; McBride, J. M. *J. Am. Chem. Soc.* **1975**, *97*, 6729. (d) Vary, M. W.; McBride, J. M. *Mol. Cryst. Liq. Cryst.* **1979**, *52*, 133.

[3] Scheffer, J. R. *Acc. Chem. Res.* **1980**, *13*, 283.

[4] Wilt, J. W. In "Free Radicals", Kochi, J. K., Ed.; Wiley: New York, 1973; Vol. 1, Chapter 8.

[5] Maillard, B.; Ingold, K. U. *J. Am. Chem. Soc.* **1976**, *98*, 1224.

0002-7863/81/1503-7069$01.25/0

chloride of T, Carlsson and Ingold estimated a rate constant of $5 \times 10^7\ s^{-1}$ for T → R at 373 K.[6] Assuming this estimate to be accurate within a factor of 2 and log A to lie between 11 and 13, one may calculate that the rate of T → R in solution at 163 K should lie between $1.5\ s^{-1}$ and $1.4 \times 10^4\ s^{-1}$. Carlsson and Ingold estimated an E_a of 7.3 kcal/mol for T → R, which with the high-temperature rate predicts a rate constant of $154\ s^{-1}$ at 163 K.

We wished to test two aspects of matrix control over T → R. First, we imagined that rearrangement might be slower than in solution, because phenyl migration would at first glance appear to require substantial atomic motion in the solid. Second, we anticipated selectivity among the three phenyl groups in solid-state rearrangement, assuming that they occupy lattice sites which are not related by symmetry. We planned to study retardation by EPR spectroscopy and selectivity by product analysis in a suitably substituted system.

In our first efforts at product analysis Pankratz found that photolysis of crystalline *tert*-butyl 3,3-diphenyl-3-*p*-chlorophenylperpropanoate (Ia) gave only the unrearranged ether (IIa) from decarboxylation and radical coupling.[7] This suggested that in the solid the alkoxy radical can move toward the T radical more readily than T can rearrange. We could not conclude that rearrangement was retarded, however, because we were unable to observe EPR signals that would have allowed measuring the rate of pair collapse. Gisler obtained similar results with several unsubstituted 3,3,3-triphenylpropanoate peresters (Ib–d).[8] To favor rearrangement we increased both the radical–radical separation and the size of the smaller radical by using symmetrical diacyl peroxides instead of peresters. Photolysis of crystalline bis(3,3-diphenyl-3-*p*-chlorophenylpropanoyl) peroxide (III) gave substantial rearrangement.[7] At least 90% of the product was rearranged, but the mixture was so complex that we despaired of more detailed analysis and mechanistic interpretation.

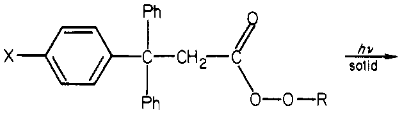

I

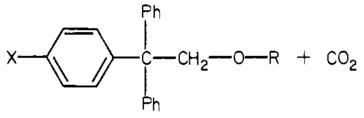

II

a, X = Cl; R = *t*-Bu
b, X = H; R = *t*-Bu
c, X = H; R = α-cumyl
d, X = H; R = 1-methylcyclohexyl

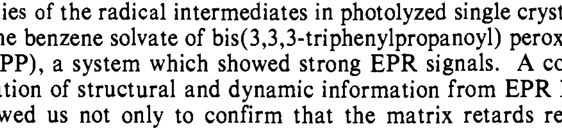

III, X = Cl
TPPP, X = H

We thus turned our attention from product analysis to spectral studies of the radical intermediates in photolyzed single crystals of the benzene solvate of bis(3,3,3-triphenylpropanoyl) peroxide (TPPP), a system which showed strong EPR signals. A combination of structural and dynamic information from EPR has allowed us not only to confirm that the matrix retards rearrangement and makes it selective but also to develop an hypothesis as to the source of the selectivity. In this paper we identify six radical-pair intermediates involved in photolysis of the benzene solvate of TPPP and discuss the kinetics of their thermal and photochemical interconversions. In the following paper we discuss the three-dimensional structures of these intermediates and what they show about the mechanism of the rearrangements and the role of neighboring molecules in determining the specificity.[9]

Scheme I

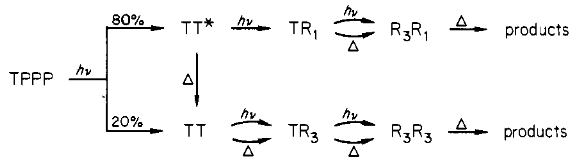

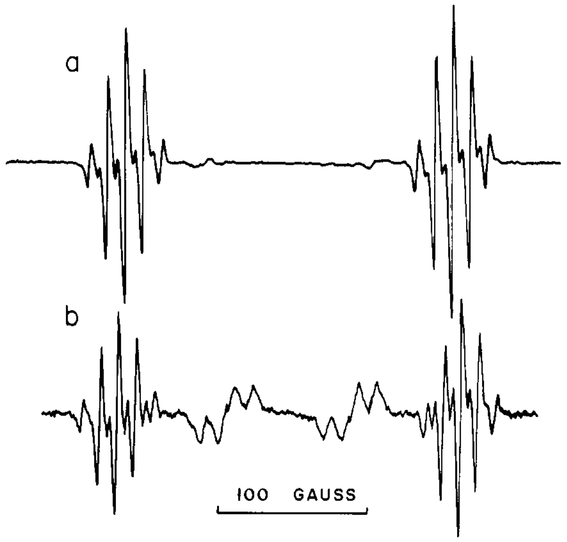

Figure 1. (a) EPR spectrum of TT* (with small amounts of TT and TR_1) obtained by photolyzing a single crystal of TPPP–benzene at 128 K. The fine-structure splitting for this crystal orientation is −219 G, and the low-field quintet is for the $T_0 \rightarrow T_1$ transition. (b) Spectrum of TT and TR_3 (with small amounts of TT* and R_3R_3) obtained by warming the crystal to 164 K for 1 min, recooling to 128 K, warming for 2 min, and recooling. In this crystal mounting the presence of R_3R_3 is indicated only by the sloping base line between the broad triplets of TR_3. Note that the fine-structure splitting for TT (−231 G) is larger than for TT*. Figure 7 in the Supplementary Material shows the spectrum after 1 min of warming.

Results and Discussion

Kinetic Scheme. EPR spectra of single crystals of the benzene solvate of TPPP, and of its methylene-deuterated (TPPP-d_4), phenyl-deuterated (TPPP-d_{30}), and fully deuterated (TPPP-d_{34}) modifications, have allowed us to establish the sequence of six radical pairs shown in Scheme I. The pairs are named according to their constituent radicals, where the subscript of R denotes which of the three phenyl groups has migrated during rearrangement, using a numbering scheme explained in the following paper. The asterisk of TT* denotes strain which is relaxed in TT.

It would have been impossible to distinguish and identify all of these intermediates in a powdered sample because of spectral overlap. Even in a single-crystal investigation it would have been very difficult except for the simplicity of the crystal lattice. Since there is only one molecule of TPPP in the unit cell, each intermediate gives a single EPR pattern for any one orientation of the crystal. Centrosymmetry of the cell makes the radicals of a pair spectroscopically indistinguishable. That is, TR gives the same spectrum as RT. Absence of centrosymmetry or presence of planes or axes of symmetry would have multiplied the patterns to give a forest of overlapping signals. Even with the $P\bar{1}$ space group, the sample orientation had to be chosen carefully for many measurements to avoid overlap. Identification of each of the six intermediates was confirmed by detailed analysis of the fine structure or zerofield splitting (zfs) and of the hyperfine splitting

---

[6] Carlsson, D. J.; Ingold, K. U. *J. Am. Chem. Soc.* **1968**, *90*, 7047.
[7] Pankratz, R. P., unpublished work in this laboratory.
[8] Gisler, M. R., unpublished work in this laboratory.
[9] Walter, D. W.; McBride, J. M. *J. Am. Chem. Soc.*, following paper in this issue.

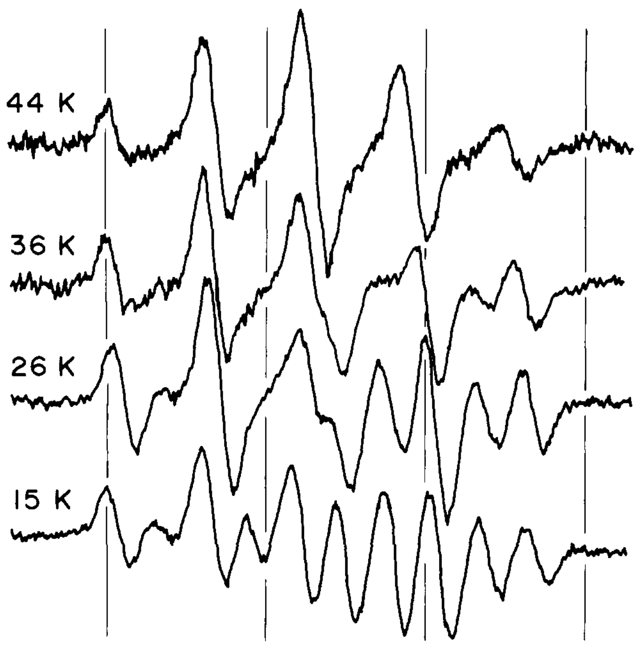

Figure 2. Effect of temperature on the $T_0 \rightarrow T_1$ quintet of TT*. The vertical grid lines are separated by 20 G. Note the shift in position of the highest field component.

(hfs), as explained in the following paper.

TT*. Brief mercury arc illumination of TPPP at 128 K with light above 300 nm, which is absorbed by the tail of the peroxide chromophore ($\epsilon_{366} = 1.7$, $\epsilon_{313} = 27$), gives the spectrum of Figure 1a. There are no peaks in the center of this spectrum, where isolated radicals should absorb. The dominant features are two sets of 1:4:6:4:1 quintets. The hyperfine quintet identifies a pair of T radicals with splitting by the four methylene hydrogens, which are rendered equivalent by rapid rotation about antiparallel Ph_3C–CH_2 bonds and by rapid electron spin exchange between the radicals of the pair.

Figure 2 shows that on cooling the quintet broadens at about 35 K and resolves into a larger number of peaks near 25 K. The free energy of activation for the process being frozen out is about 0.7 kcal/mol, but it is not obvious what the process is. If it were 180° rotation of the methylene group which averages the hfs, the outermost peaks would not be expected to split, as one of them is observed to do. If it were an oscillation in the relative positions of the two methylene groups in the radical pair which averages the zfs, the double-minimum potential with energy minima separated by only about 0.05 Å would be remarkable.

Spin exchange in the triplet-state pair explains why the hfs constant is just half as large as in isolated R–CH_2 radicals.[2c] The zfs between the two quintets is due to electron–electron magnetic dipole interaction between the two radicals. At no temperature have we seen spectra attributable to acyloxy radicals, analogous to the benzoyloxyl radicals we have studied previously.

TT. Figure 1a also shows a weaker pair of quintets interleaving the quintets of TT*. After low-temperature photolysis the weak quintets are about one-fourth as strong as those of TT*, but annealing at 150–160 K causes them to grow at the expense of TT* (see Figure 1b). The same arguments which identify TT* also identify TT. Because TT* and TT differ slightly in the separation of their radical centers, they may be distinguished by the difference in zfs.

TR$_3$. Figure 1b also shows the growth of a pair of ill-resolved triplets as TT* anneals to TT. The zfs is smaller than in the TT pairs, and the magnitude and multiplicity of the hfs shows that one only of the original T radicals persists in this new pair. Complete deuteration of the aromatic rings narrows the lines to give a well-resolved triplet of quartets, where the quartet splitting results from smaller additional hfs of two inequivalent hydrogens (see Figure 8, Supplementary Material). Deuteration of the methylene hydrogens (TPPP-d_4) leaves broad singlets only. If one radical in the TT pair had undergone neophyl rearrangement, this behavior would be expected, assuming conformational inequivalence of the β-methylene hydrogens of R in the solid and delocalization of the odd electron into two of the phenyl groups, the hydrogens of which give unresolved splitting. In fully deuterated material (TPPP-d_{34}), where the signal may be identified by its zfs, TR$_3$ was observed after extended illumination at a temperature too low for it to have been formed thermally from TT (see Figure 3).

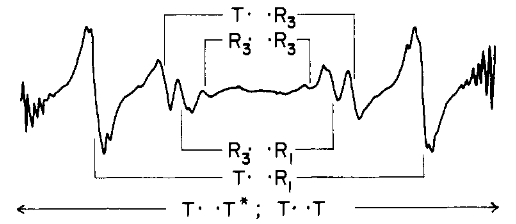

Figure 3. Signal from a crystal of TPPP-d_{34} after 5 min photolysis at 102 K. The intense, complex, overlapping patterns from deuterated TT* and TT pairs continue right and left from the region shown. Although the TR$_3$ and R$_3$R$_3$ peaks are weak in this spectrum, they grow dramatically on warming the photolyzed crystal. Note that all peaks may be assigned to one of the six radical pairs discussed in the text.

R$_3$R$_3$. Continued warming of a crystal from which TT* and TT had disappeared resulted in disappearance of TR$_3$ and appearance of a pair of broad singlets with no resolvable hfs. Even in partially deuterated samples no recognizable hfs was resolved. Such complex hfs would be expected for a pair of rearranged radicals, but identification of this intermediate as R$_3$R$_3$ rests primarily on chemical plausibility and analysis of the zfs tensor. The zfs shows that one of the radicals is R$_3$ but does not distinguish clearly between R$_1$ and R$_3$ for the other.[9] As in the case of TR$_3$, a weak signal for R$_3$R$_3$ appeared after prolonged illumination of TPPP-d_{34} at low temperature (Figure 3). The signal of R$_3$R$_3$ persists with changes too subtle for the present analysis to interpret as the crystal is warmed to 200 K, at which temperature it decays without free-radical progeny.

TR$_1$. Figure 1a shows a pair of very weak, broad signals with zfs about half as large as those of TT* and TT, but similar to that of TR$_3$. Prolonged illumination at 102 K makes this signal grow as TT* approaches a photostationary concentration. The signal appears at the most intense doublet in Figure 3. In TPPP-d_{30} the hfs pattern is a triplet of doublets. The triplet spacing is like that of the TT quintet, confirming that one radical in the pair is T. Analogy with TR$_3$ in zfs, genesis, and reactivity suggests that the radical paired with T has undergone neophyl rearrangement. Since hfs by only one methylene hydrogen of R can be resolved, the conformation of the R radical must be such as to give the second methylene hydrogen a very small hfs.

R$_3$R$_1$. Continued photolysis or warming of a TPPP-d_{34} crystal containing a substantial TR$_1$ signal gives another doublet with weak zfs, which cannot be observed after photolysis at a temperature where TT* $\rightarrow$ TT is rapid or after warming a lightly illuminated crystal (see Figure 3). At 250 K the signal decays without free-radical progeny. Identification of this signal as R$_3$R$_1$ rests on analogy in zfs, genesis, and reactivity with R$_3$R$_3$. The zfs evidence is not unambiguous as to the index of the first R, although the second is clearly R$_1$.[9]

Dynamics of Thermal Processes. There are three obstacles to rigorous rate determination for the thermal processes initiated by photolysis of TPPP. First, overlapping of peaks from several intermediates complicates the standard problems of quantitative EPR. In most cases overlap can be reduced or eliminated by appropriate crystal mounting and isotopic substitution. Second, in the solid state a nominally first-order process may become a composite of processes at a number of subtly different lattice sites, each with its own first-order rate constant.[10] This problem is especially acute in crystals which have suffered extensive (several

---

(10) For example, see: Mikhailov, A. I.; Lebedev, Ya. S.; Buben, N. Ya. *Kinet. Katal.* **1964**, *5*, 1020.

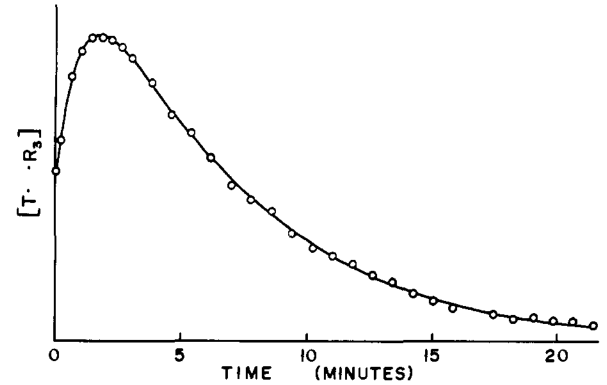

Figure 4. Time development of the signal of TR_3 at 163 K after brief photolysis. The shape of the line was adjusted with one rate parameter to fit the experimental points and establish the rate constant for decay of TR_3 in Table II (see supplementary material).

Table I. Activation Parameters for Radical Pair Decay

species	$\log A$, s^{-1}	E_a, kcal/mol	T^a
TT*	11.2	9.6	160
TT	12.0	10.6	166
TR_1	9.7	8.8	165
TR_3	11.5	10.4	169
R_3R_3	14	15	204
R_3R_1	11	16	256

[a] Temperature (K) which gives a half-life of 1 min.

percent) decomposition. Third, some of the steps of Scheme I seem not to be quantitative. Leakage to diamagnetic products from several of the intermediates is consistent with the apparent complexity of product mixtures.

We tested for leakage by double integration of sequential spectra for the simplest case of intermittent warming after brief photolysis at low temperature (see Figure 9, Supplementary Material). Although the intial stages of TT* → TT → TR_3 appear to proceed in high yield (>80%, judging by the rate at which the overall signal decays), the yield of R_3R_3 from TR_3 seems to be significantly less than 50%. Since it is unclear whether the portion of TR_3 decay which yields other products involves rearrangement or not, the rate of this decay which yields other products involves rearrangement or not, the rate of this decay gives only an upper limit for the rate of neophyl rearrangement of the TR_3 pair. The same may be true for $TR_1 \rightarrow R_3R_1$. Because we can observe ESR signals from appreciable amounts of the RR pairs, we do not think the rates are overestimated by a factor as large as 4.

The rates at which various signals decayed were monitored by the peak-to-peak or base-line-to-peak amplitude of derivative spectra with crystal orientation chosen to minimize spectral overlap. There were no systematic differences between rates measured by repeated scanning and those measured by fixing the magnetic field to observe decay of a single peak, and both techniques were employed. Fresh crystals were used for rate studies and chemical conversion was kept small, much less than 0.1%.

Scheme I suggests that in the dark both TT* and TR_1 should decay exponentially, and in fact first-order plots of signal amplitude were linear for 2 to 3 half-lives. Similar plots for R_3R_1 and R_3R_3 were also linear for 2 half-lives, because their precursors live less than 0.1 s at the temperature of measurement. In all of these cases decay slowed in its final stages, as would be expected for a sample with a small number of sites in which reaction is atypically slow. Decay of TT and of TR_3 is complicated by their simultaneous formation from TT* and TT, respectively. For these intermediates the amplitude–time data were fitted to sums of two or three decaying exponentials, respectively, by varying the pre-exponential factors and one of the exponential coefficients of time (the others being fixed by previously determined precursor rate constants). During decay of 95% of TR_3 the signal amplitude was fitted within 2% of its maximum, while experimental uncertainty was estimated at 5% of that value (see Figure 4). Precision of the fit for TT was comparable. A composite Arrhenius plot for first-order decay of these six intermediates is presented in Figure 5, and the activation parameters appear in Table I. The observed rate constants are presented in Table II, Supplementary Material.

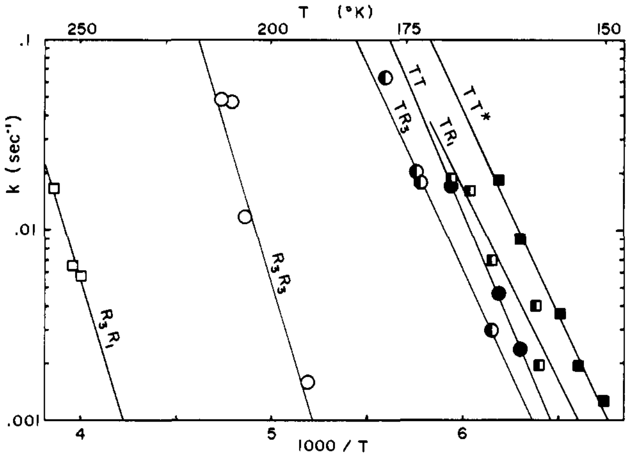

Figure 5. Arrhenius plot of the first-order rate constants for Table II (see supplementary material).

The six processes for which we have estimated thermal rates fall into three mechanistic classes: relaxation (TT* → TT), neophyl rearrangement (TT → TR_3, $TR_1 \rightarrow R_3R_1$, and $TR_3 \rightarrow R_3R_3$), and radical-pair collapse (R_3R_1 or R_3R_3 → products). The first two classes have activation energies near 10 kcal/mol, while pair collapse has E_a about 15 kcal/mol. It was noted above that some type of pair collapse seems to compete with at least one of the rearrangements. For this collapse E_a must be much closer to 10 than to 15 kcal/mol.

Our data do not justify detailed interpretation of activation parameters, but it is clear that neophyl rearrangements in the matrix are significantly slower than they would be in solution. According to the range estimated in the introduction for the rate in solution at 163 K, the matrix retards rearrangement by at least one hundred-fold and perhaps by as much as one million-fold. Unfortunately we cannot estimate the solution rate more precisely. The E_a for solid-state rearrangement is 1.5 to 3 kcal/mol greater than Carlsson and Ingold's estimate for rearrangement in solution. Among the three solid-state rearrangements at 163 K there are rate energy differences as much as a factor of 2 or 3, corresponding to activation free energy differences of 0.2–0.4 kcal/mol. Since the slowest rate ($TR_3 \rightarrow R_3R_3$) is an upper limit, the rate difference could be twice as large.

Although one might have anticipated that lattice rigidity would be reduced by the first rearrangement so that the second rearrangement from a pair of T radicals in the solid would be faster than the first, the rate of TT rearrangement is in fact intermediate between those of TR_3 and TR_1. On the other hand, thermal rearrangement of TT* does not compete with its relaxation to TT, and this relaxation is only slightly faster that rearrangement of TR_1 (see Figure 5).

The activation energy for collapse of pairs of smaller radicals in photolyzed diacyl peroxides is usually much less than 10 kcal/mol.[2d] It is tempting to attribute the high E_a for the RR pairs to the size and rigidity of the radicals, but the increase in distance between the radical centers during rearrangement is probably at least as important.

Photochemical Reactions. Scheme I includes five photochemical steps. The first is double decarboxylation of the diacyl peroxide. Such processes are well precedented,[11] and our observations add little to the knowledge on their degree of simultaneity. We observed no signals attributable to acyloxyl radicals. We made no attempt to monitor quantum yields. Photolysis by 366-nm light suggests that reaction is stimulated through absorption by the tail of the peroxide chromophore, and separation of these chromo-

---

(11) Sheldon, R. A.; Kochi, J. K. *J. Am. Chem. Soc.* **1970**, *92*, 4395.

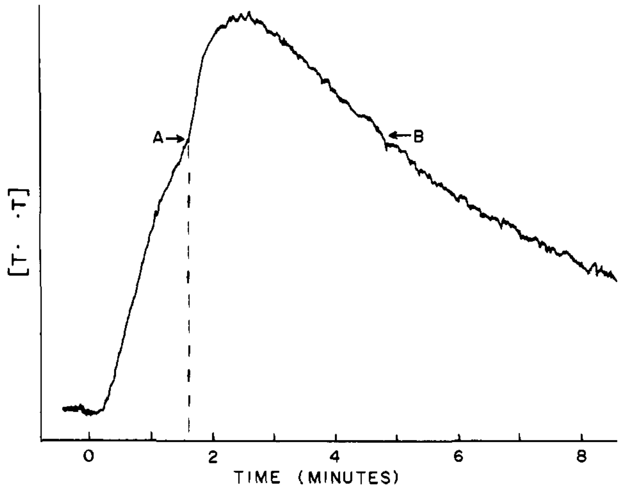

Figure 6. Time development of the signal of TT at about 163 K. Photolysis began at 0 min and was stopped at 1.6 min (A). Comparison of the slope at B with the change of slope at A shows that during photolysis more than half of the decay of TT is photochemical.

phores by more than 9.8 Å in the crystal suggests that excitation remains localized in the absorbing molecule. If excitation remains localized, decomposition probably occurs randomly throughout the crystal, since light is absorbed randomly. On the basis of the solution extinction coefficient a crystal thickness of 3.6 mm would be required to absorb 90% of incident 366-nm light. For 313-nm light the required thickness is 0.2 mm. Of course after long photolysis, surface reactions could be favored because of light attenuation by product molecules.

Each of the other four photochemical steps involves neophyl rearrangement. It is remarkable that in the three cases where a certain precursor gives both thermal and photochemical rearrangement, the products of the two reaction modes are identical. Photochemical rearrangement does not result simply from local heating during low-temperature photolysis, however, because it can be induced without inducing motion from TT* to TT, and because the TR_1 product cannot be formed thermally. Figure 3 and analogous spectra for different crystal mountings show only the six radical pairs of Scheme I, although many others could be imagined, such as TR_2, R_1R_1, R_2R_1, and R_2R_3.

The peculiar kinetic profiles of TT and TR_3 confirm that photolysis is involved in their decay. Figure 6 shows the profile for TT before, during, and after a 1.6-min period of photolysis at 163 K. After an induction period of about 15 s, during which TT* builds up, TT rises rapidly then begins to depart from linearity as it approaches its photostationary concentration. When photolysis is interrupted, one might have anticipated that decay of the TT signal would be delayed for a comparable induction period, during which TT* is depleted. But instead of halting at a plateau, the amount of TT increases temporarily, and in fact it grows *faster* than just before photolysis was interrupted. This is because it is being formed from TT* at the same rate as it was during illumination, but it is no longer being depleted by photorearrangement. If one assumes that temperature changes are negligible, the change in slope at point A corresponds to the change in decay rate when the light is extinguished, that is, presumably, to minus the rate of photorearrangement. The slope at point B corresponds to the thermal decay rate of the same amount of TT after substantial depletion of TT*. The slope at B is only about one-third of the change in slope at A, so that even making allowance for small temperature differences, rearrangement at this temperature and light intensity is predominantly photochemical.

We remain puzzled about what chromophore is responsible for this reaction. It is not obvious how T itself would absorb at relatively long wavelengths. Sensitization by a neighboring peroxide group, with an oxygen atom 3.56 Å from the para carbon of one of the phenyl groups of T, may be conceivable and could explain why color filters did not permit varying the relative rates of decarboxylation and rearrangement.

Experimental Section

EPR Measurements were made with a Varian E-9 spectrometer operating at X-band with an E-231 multipurpose cavity and 100 kHz detection. Microwave power was kept below the threshold for saturation, typically 0.2 mW at 60 K. The peroxide crystals (typically 2.5 × 2.5 × 0.7 mm) were mounted with Dow-Corning high-vacuum silicone grease on a Suprasil quartz rod and cooled by a stream of nitrogen (or helium) controlled within ±1 K by Varian V-4540 (or Airco Helitran) cryostats. The temperature was monitored by copper–constantan (or gold–chromel) thermocouples. Double integration was performed on digitized data from an analogue trace. The base line slope of the derivative curve was adjusted to make the absorption spectrum return to base line beyond the signal.

Photolysis was by an Osram HBO 200w/2 high-pressure mercury arc focussed by an *f*/1 quartz lens and filtered by 5 cm of a 0.4 M $CuSO_4$ solution to remove IR and UV below 300 nm. Wavelengths longer than 390 nm did not decompose the peroxide. In some experiments a series of Corning color filters was used in an unsuccessful attempt to generate TT* without TR_1.

3,3,3-Triphenylpropanoyl peroxide and its deuterated analogues were prepared and crystallized from benzene by routine procedures described in the Supplementary Material.

Acknowledgment. This work was supported by the National Science Foundation (DMR 76-01996). The EPR spectrometer was obtained with the aid of an NSF departmental instrument grant. J.M.M. is grateful for the hospitality of Professor J. M. Thomas, University of Cambridge, and for a Senior Visiting Fellowship from the Science Research Council of Great Britian during preparation of this manuscript.

Supplementary Material Available: Experimental details, thermal decay rates, and Figures 7–9 (6 pages). Ordering information is given on any current masthead page.